Supporting Information

Water-in-Salt Electrolyte Achieves High Energy Density at Ultralow-Temperature for Aqueous Symmetrical Supercapacitors

Jiajing Zhu,[a] Yi Sun,[a] Jie Gao,[a] Zhanbin Qin,[a] Yanan Zhou,[a] Ran Tian [a*] and Yun Gao [a*]

*E-mail: gaoyun@ncst.edu.cn; 943525900@qq.com

Experimental Section

1. Preparation of electrolytes and electrodes

Aqueous electrolytes were prepared by molality (mol-salt in kg-solvent) of bis(trifluoromethane)sulfonimide lithium salt ($LiN(CF_3SO_2)_2$, LiTFSI) (>98%) and deionized water. The electrolyte concentration involves 1, 5, 7, 8, 9, 10, 11, 12, 13, 14, 16, 18 and 21 mol kg^{-1}. Among them, the molar ratios of H_2O to LiTFSI in several important concentrations are 55.56 (1 mol kg^{-1}), 11.11 (5 mol kg^{-1}), 7.94 (7 mol kg^{-1}), 6.17 (9 mol kg^{-1}), 5.56 (10 mol kg^{-1}), 4 (13.9 mol kg^{-1}), 3.97 (14 mol kg^{-1}), 2.65 (21 mol kg^{-1}), and 1.63 (34 mol kg^{-1}), respectively.

The electrodes were fabricated by compressing activated carbon (AC, YP-50F), acetylene black (AB), poly(tetrafluoroethylene) (PTFE) binder at the weight ratio of 8:1:1 on nickel foam. The electrode sheet was pressed flat after drying in a vacuum oven at 80 °C for 12 h to remove the dispersant N-methylpyrrolidone (NMP). The size of the electrodes in the three-electrode system is a square with a side length of 1 cm, but it is a 1 cm diameter circle in the symmetric supercapacitor.

2. Characterization and electrochemical measurements

Differential scanning calorimetry (DSC) of the different LiTFSI concentration electrolytes were obtained on a DSC8000. Samples were exposed to a cooling/heating cycle from 30 °C to -60 °C to 50 °C at 2 °C min^{-1}, and standing at -60 °C for 1 h. Fourier transform infrared spectrometer (FTIR) spectra were collected in the range of 400~4000 cm^{-1} through Thermo fisher iN10 & iZ10. The ionic conductivity of aqueous electrolytes was tested by Seven Excellence at room and low temperature.

The electrochemical stability windows of various electrolytes were measured with a typical three-electrode system by using activated carbon electrode, Ag/AgCl electrode and Pt electrode as the working, reference and counter electrode, respectively. Enclosing two activated carbon electrodes in a

CR2032-type coin cell and injecting with different types of LiTFSI/H_2O electrolytes to assemble symmetric supercapacitors, and glass microfiber filters (GF/D) served as the separators. Linear sweep voltammetry (LSV), cyclic voltammetry (CV) and electrochemical impedance spectroscopy (EIS) were performed on CHI660E electrochemical work station (Shanghai, China), and at each set temperature the sample was stood for at least 2 h before test. LSV was conducted at a scan rate of 0.5 mV s^{-1} to evaluate the electrochemical window of the electrolyte on an activated carbon working electrode. The CV curves of the supercapacitors were recorded at various scan rates and temperatures over the potential range from 0 V to the maximum voltage. EIS measurements were performed in the frequency range of 0.01~10^5 Hz with an amplitude of 5 mV. The galvanostatic charge/discharge (GCD) was carried out on Land CT2001A battery test system (Wuhan, China) using symmetrical activated carbon-based supercapacitors.

The specific capacitance C (F g^{-1}) of the supercapacitors was calculated from CV curve by equation (1):

$$C = \frac{\int_{V_l}^{V_u} i\mathrm{d}V}{2mv\Delta V} \tag{1}$$

Where V_l (V) and V_u (V) is respectively the lower and upper limits of the operating potential, $i\mathrm{d}V$ (AV) is the area of the CV curve, m (g) is the mass of active material on one electrode, v (V s^{-1}) is scan rate, ΔV (V) is the operation voltage.[1]

The energy density E (Wh kg^{-1}) of the supercapacitors was defined as follows:

$$E = \frac{C\Delta V^2}{7.2} \tag{2}$$

Results and Discussion
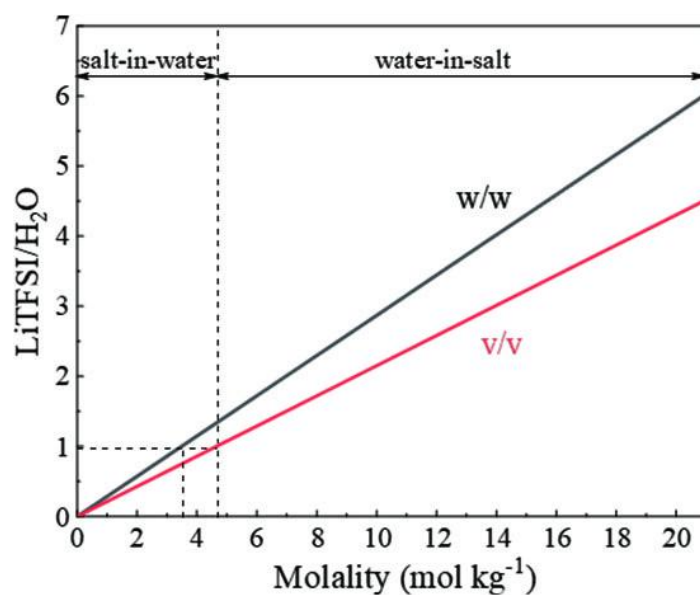
Fig. S1 The weight and volume ratio of LiTFSI to H_2O change with increasing the molarity of LiTFSI in H_2O.
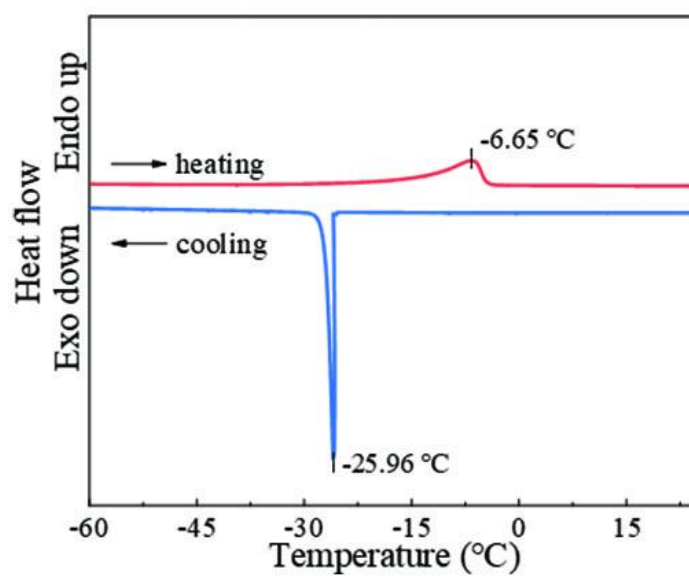
Fig. S2 The DSC curves of cooling and heating at 1 mol kg^{-1} LiTFSI/H_2O.
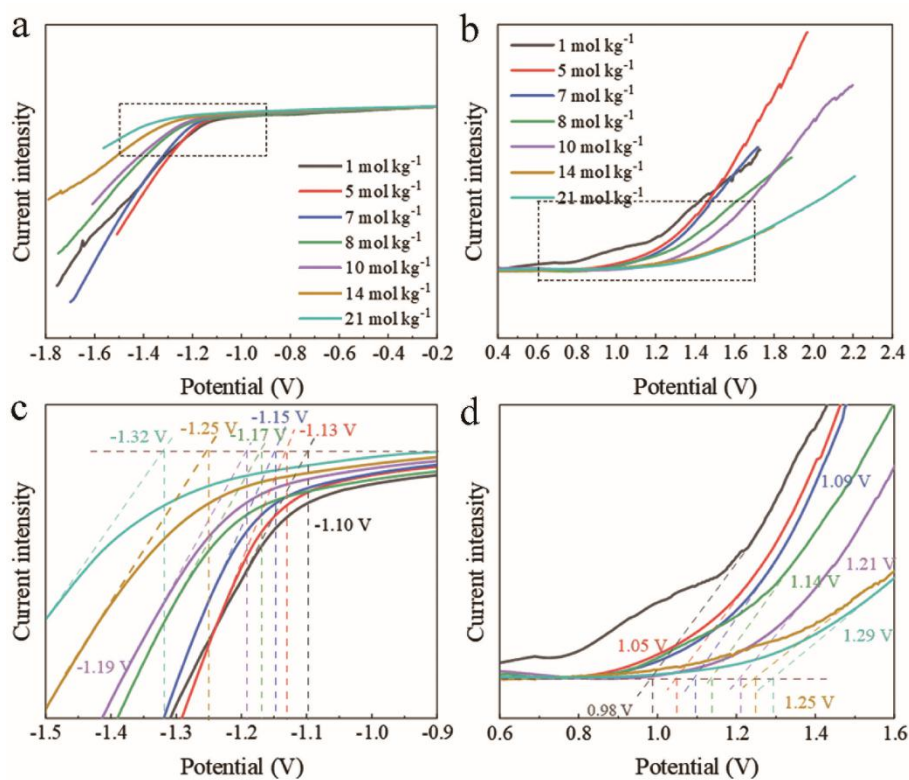
Fig. S3 LSV curves of the LiTFSI/H$_2$O electrolyte with different concentrations as measured on activated carbon electrodes at 0.5 mV s^{-1} and 0 °C.
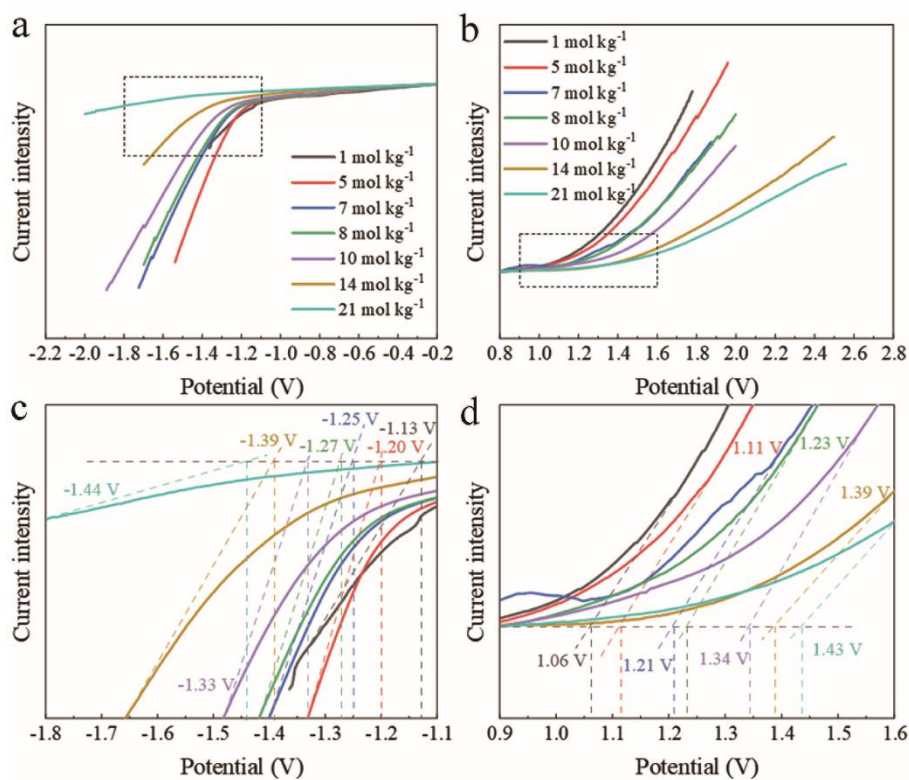
Fig. S4 LSV curves of the LiTFSI/H$_2$O electrolyte with different concentrations as measured on activated carbon electrodes at 0.5 mV s^{-1} and -10 °C.
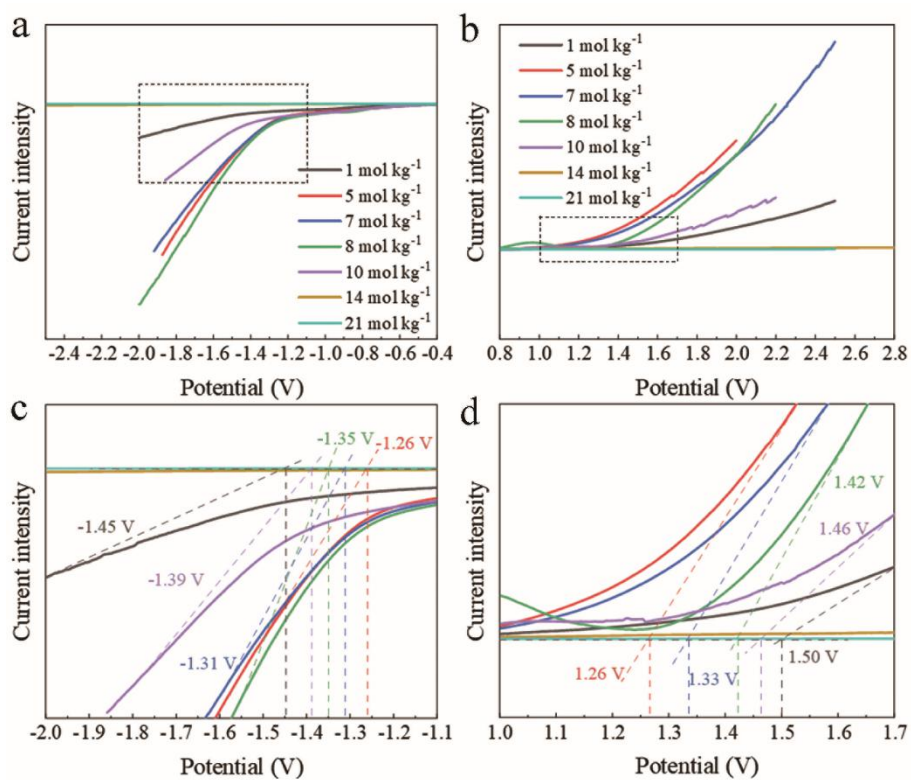
Fig. S5 LSV curves of the LiTFSI/H$_2$O electrolyte with different concentrations as measured on activated carbon electrodes at 0.5 mV s^{-1} and -20 °C.
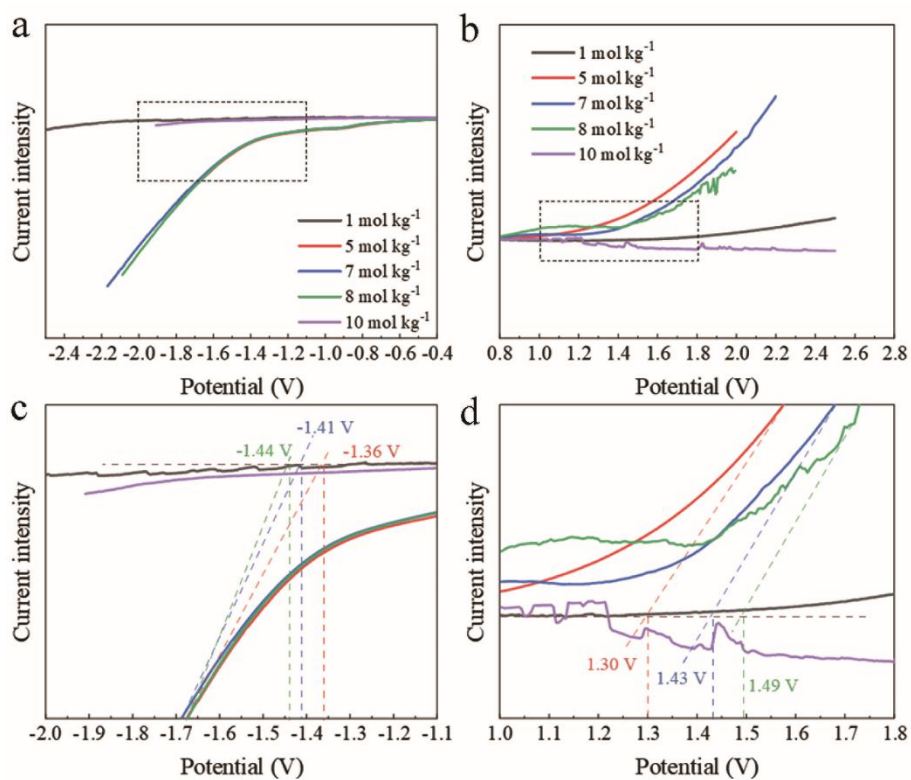
Fig. S6 LSV curves of the LiTFSI/H$_2$O electrolyte with different concentrations as measured on activated carbon electrodes at 0.5 mV s^{-1} and -30 °C.
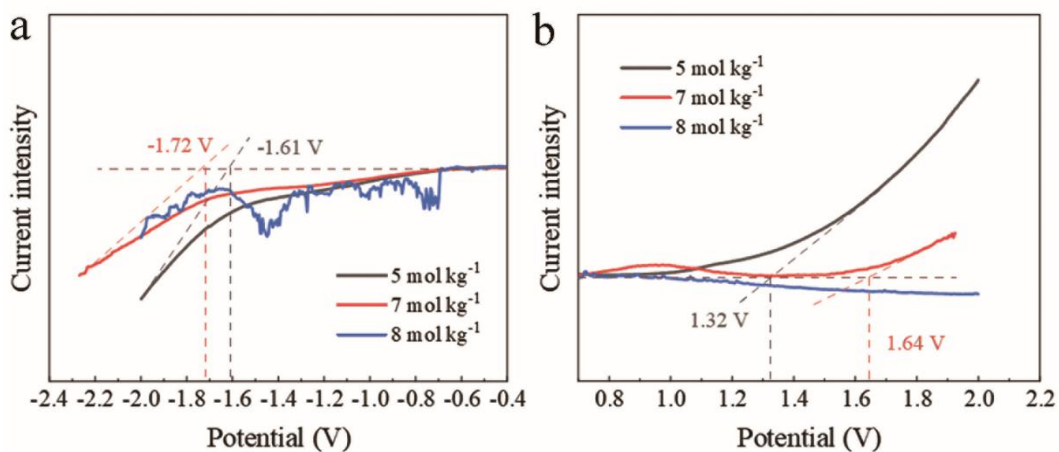
Fig. S7 LSV curves of the LiTFSI/H$_2$O electrolyte with different concentrations as measured on activated carbon electrodes at 0.5 mV s^{-1} and -40 °C.
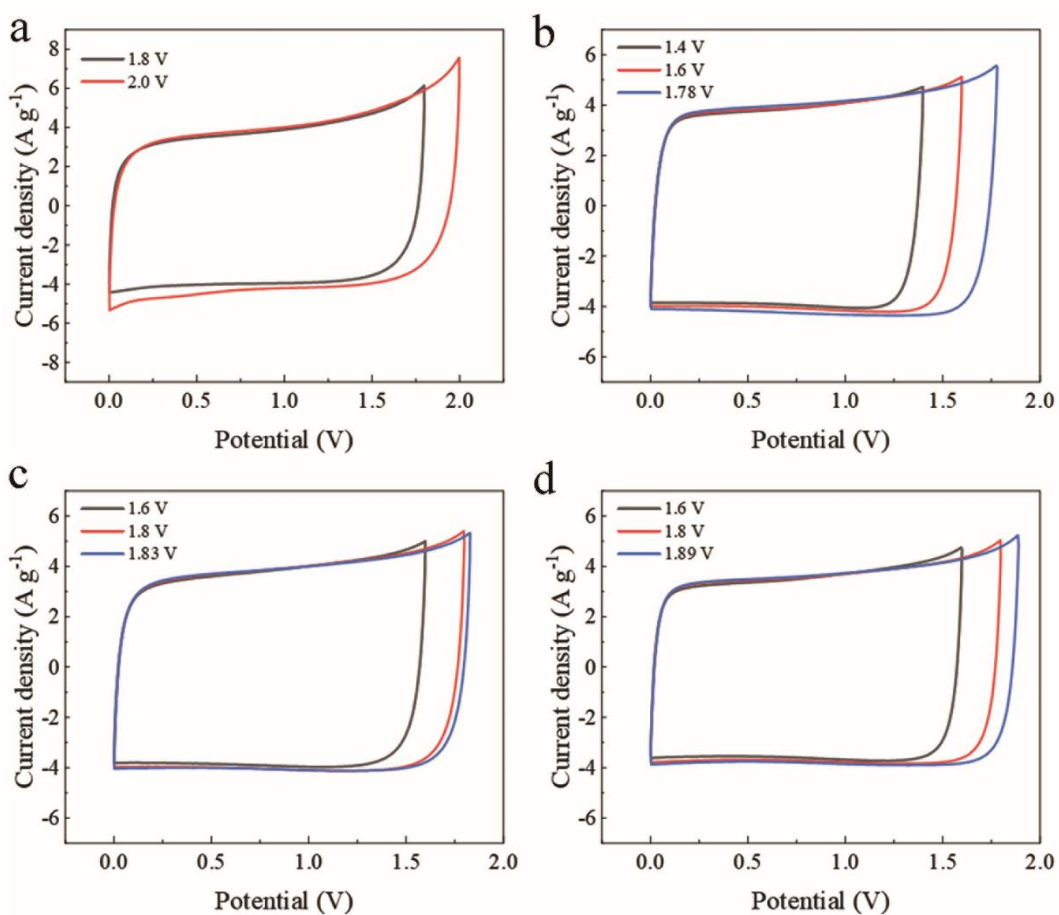
Fig. S8 CV curves of the supercapacitor using LiTFSI/H$_2$O electrolyte with different concentrations and voltage at 100 mV s^{-1} under 25 °C: a) 1 mol kg^{-1}, b) 5 mol kg^{-1}, c) 7 mol kg^{-1} and d) 8 mol kg^{-1}.
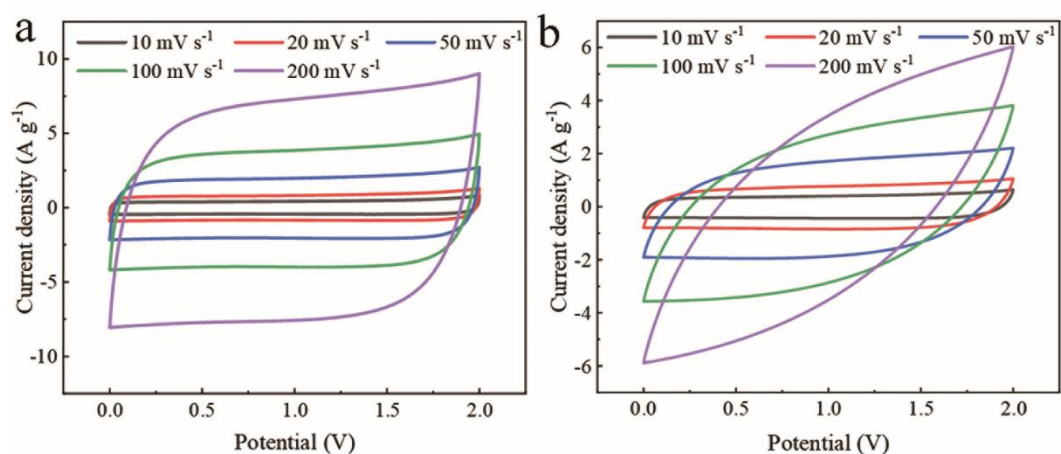
Fig. S9 CV curves of the supercapacitor using a) 14 mol kg^{-1} and b) 21 mol kg^{-1} LiTFSI/H$_2$O with different scanning rates at an operation voltage of 2.0 V.
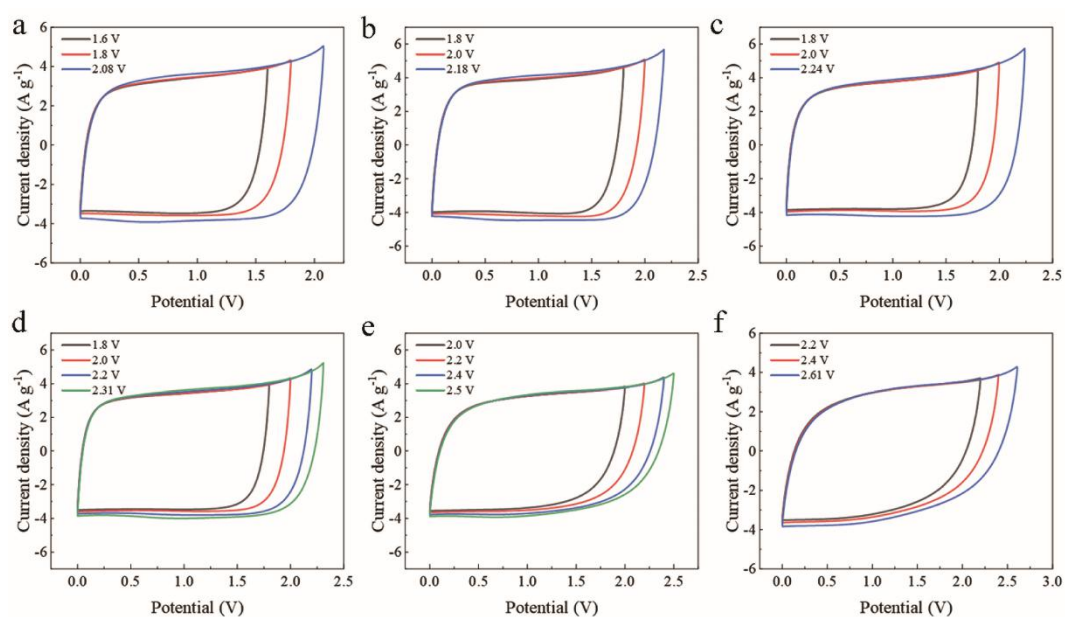
Fig. S10 CV curves of the supercapacitor using LiTFSI/H$_2$O electrolyte with different concentrations and working voltage at 100 mV s^{-1} under 0 °C: a) 1 mol kg^{-1}, b) 5 mol kg^{-1}, c) 7 mol kg^{-1}, d) 8 mol kg^{-1}, e) 14 mol kg^{-1} and f) 21 mol kg^{-1}.
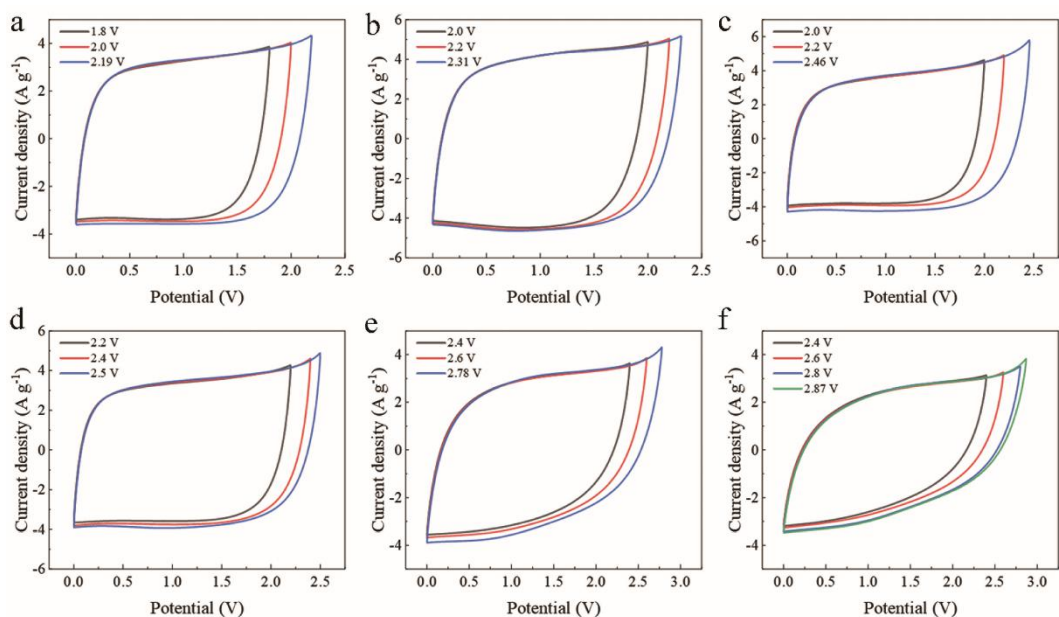
Fig. S11 CV curves of the supercapacitor using LiTFSI/H₂O electrolyte with different concentrations and working voltage at 100 mV s⁻¹ under -10 °C: a) 1 mol kg⁻¹, b) 5 mol kg⁻¹, c) 7 mol kg⁻¹, d) 8 mol kg⁻¹, e) 14 mol kg⁻¹ and f) 21 mol kg⁻¹.
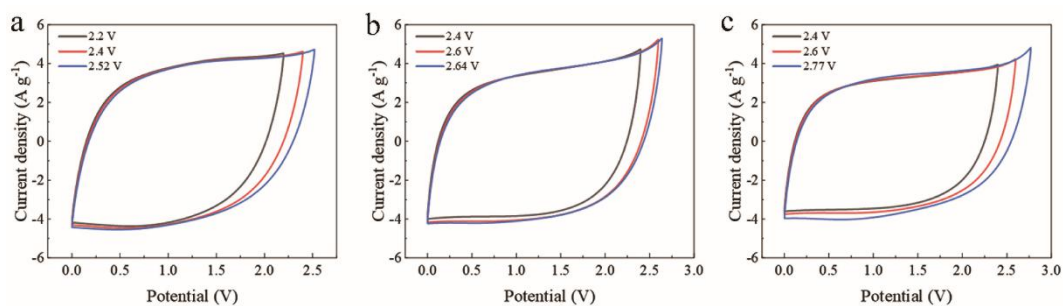
Fig. S12 CV curves of the supercapacitor using LiTFSI/H₂O electrolyte with different concentrations and working voltage at 100 mV s⁻¹ under -20 °C: a) 5 mol kg⁻¹, b) 7 mol kg⁻¹ and c) 8 mol kg⁻¹.
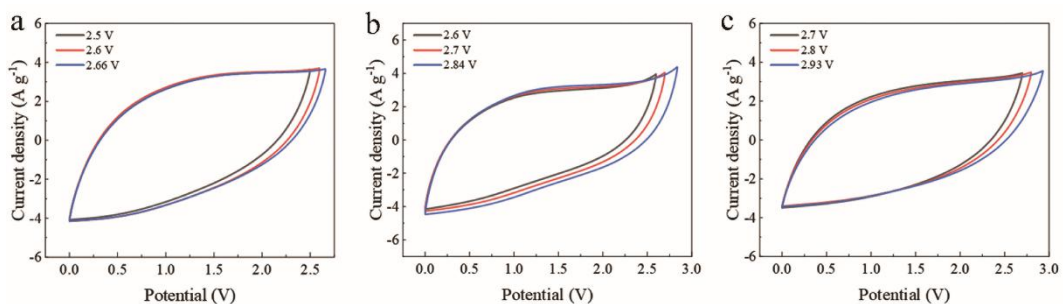
Fig. S13 CV curves of the supercapacitor using LiTFSI/H₂O electrolyte with different concentrations and working voltage at 100 mV s⁻¹ under -30 °C: a) 5 mol kg⁻¹, b) 7 mol kg⁻¹ and c) 8 mol kg⁻¹.
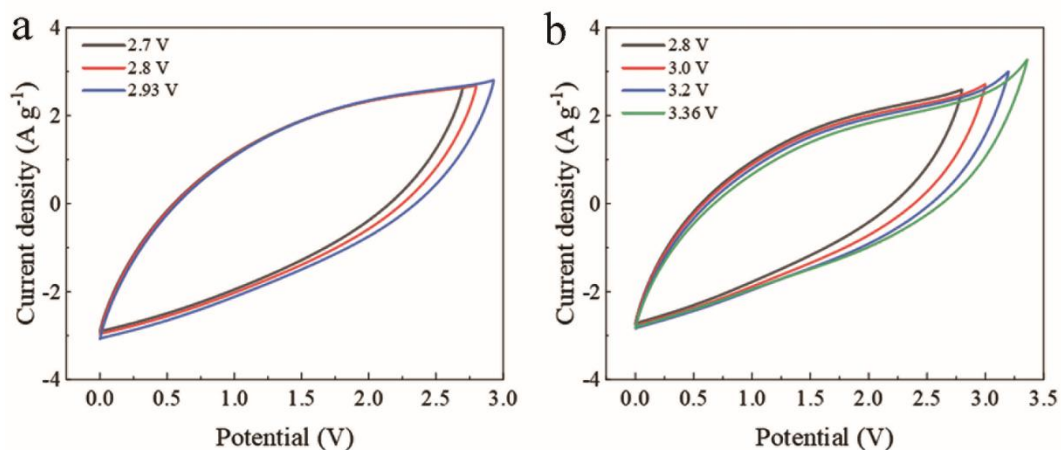
Fig. S14 CV curves of the supercapacitor using LiTFSI/H_2O electrolyte with different concentrations and working voltage at 100 mV s^{-1} under -40 °C: a) 5 mol kg^{-1} and b) 7 mol kg^{-1}.
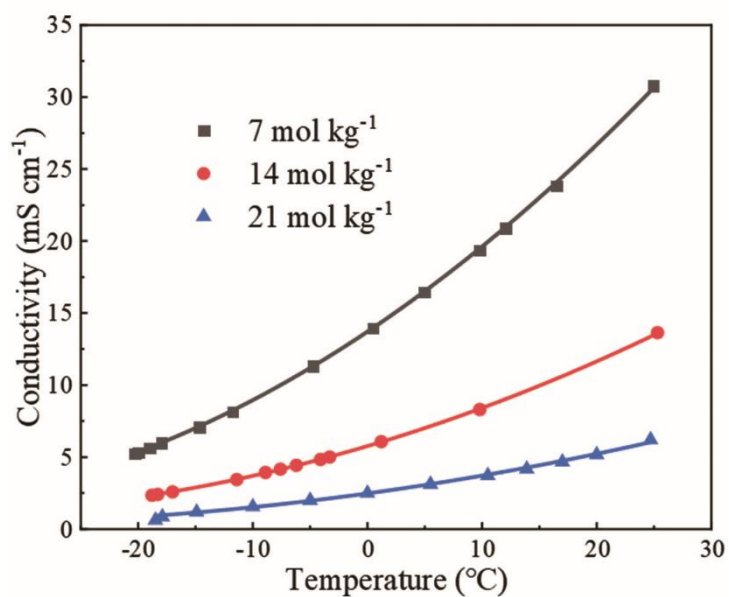
Fig. S15 The ionic conductivity of the LiTFSI/H_2O electrolyte under low temperature with different concentrations.
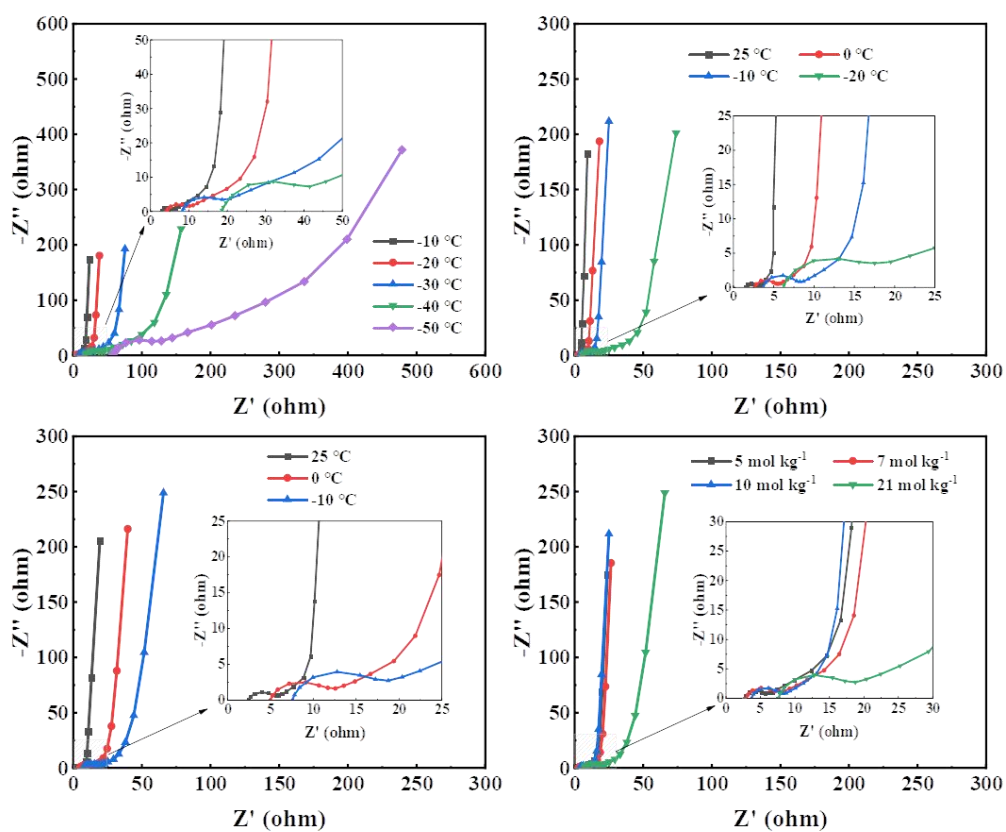
Fig. S16 Nyquist impedance plots of the LiTFSI/H$_2$O electrolyte under 25 °C and low temperature with different concentrations: a) 5 mol kg^{-1}, b) 10 mol kg^{-1}, c) 21 mol kg^{-1} and d) -10 °C.
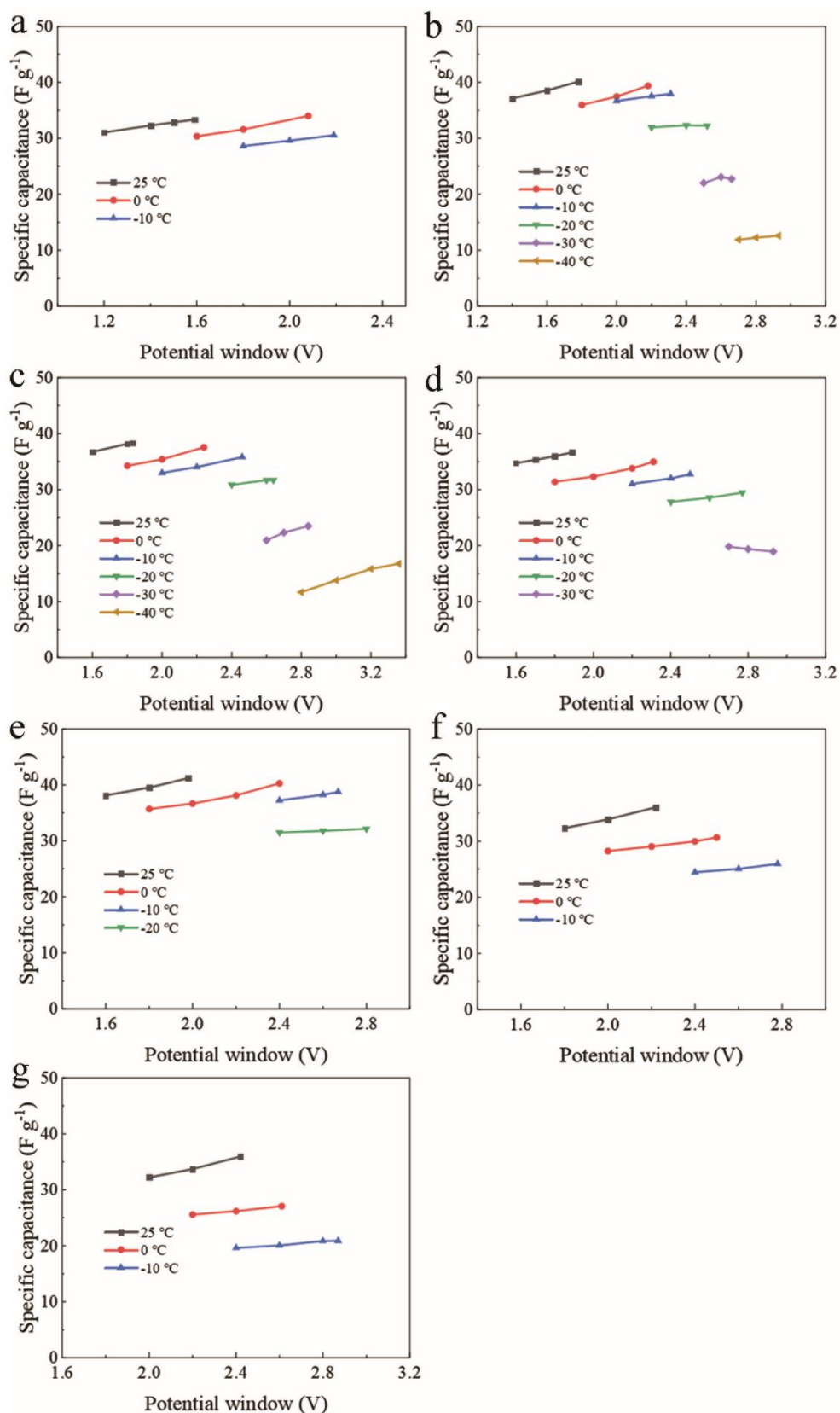
Fig. S17 The specific capacitance of the supercapacitor using LiTFSI/H$_2$O electrolyte with different concentrations and temperatures: a) 1 mol kg^{-1}, b) 5 mol kg^{-1}, c) 7 mol kg^{-1}, d) 8 mol kg^{-1}, e) 10 mol kg^{-1}, f) 14 mol kg^{-1} and g) 21 mol kg^{-1}.
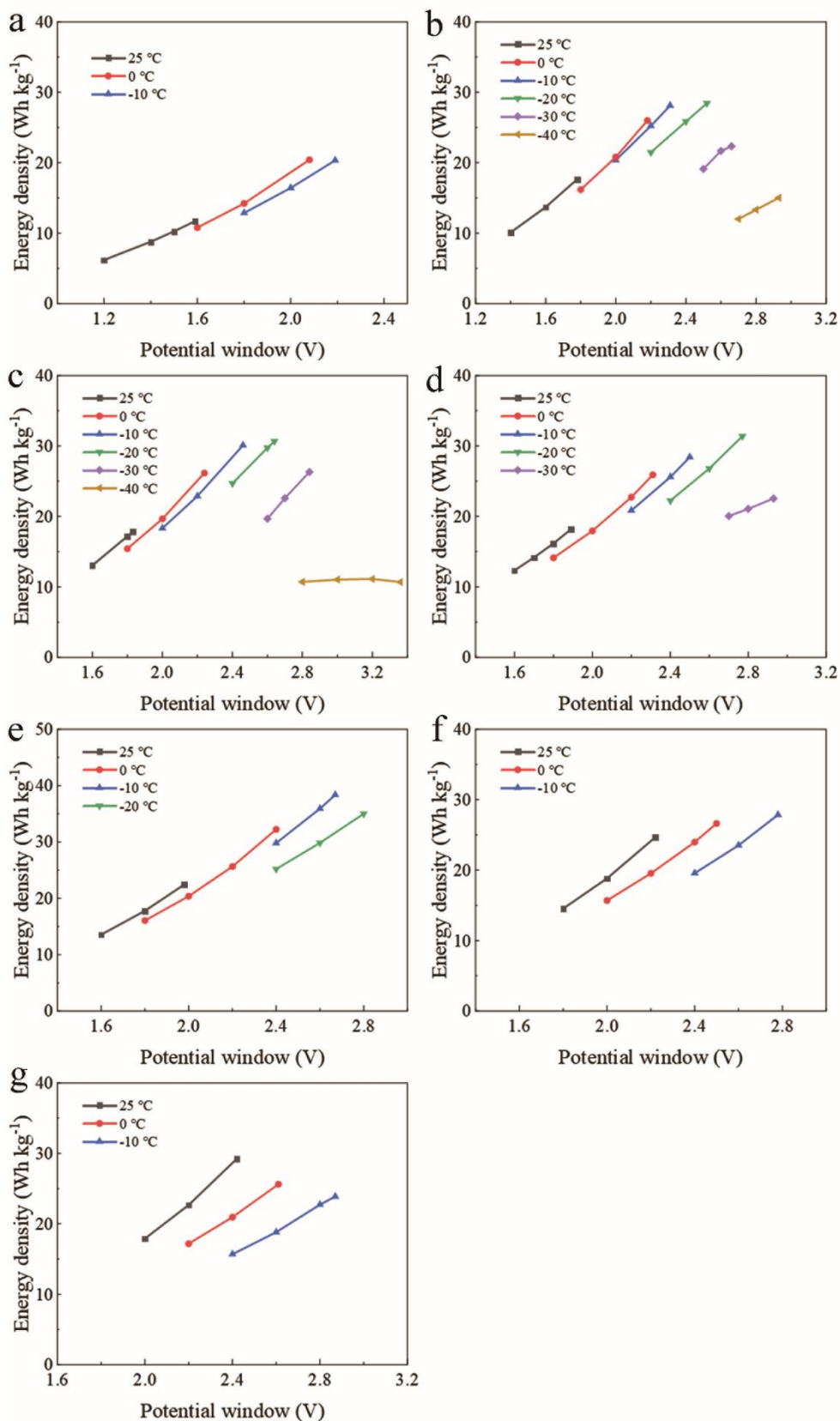
Fig. S18 The energy density of the supercapacitor using LiTFSI/H_2O electrolyte with different concentrations and temperatures: a) 1 mol kg^{-1}, b) 5 mol kg^{-1}, c) 7 mol kg^{-1}, d) 8 mol kg^{-1}, e) 10 mol kg^{-1}, f) 14 mol kg^{-1} and g) 21 mol kg^{-1}.

Fig. S19 The optical photograph of 8 mol kg^{-1} LiTFSI/H$_2$O electrolyte after LSV test at -40 °C.
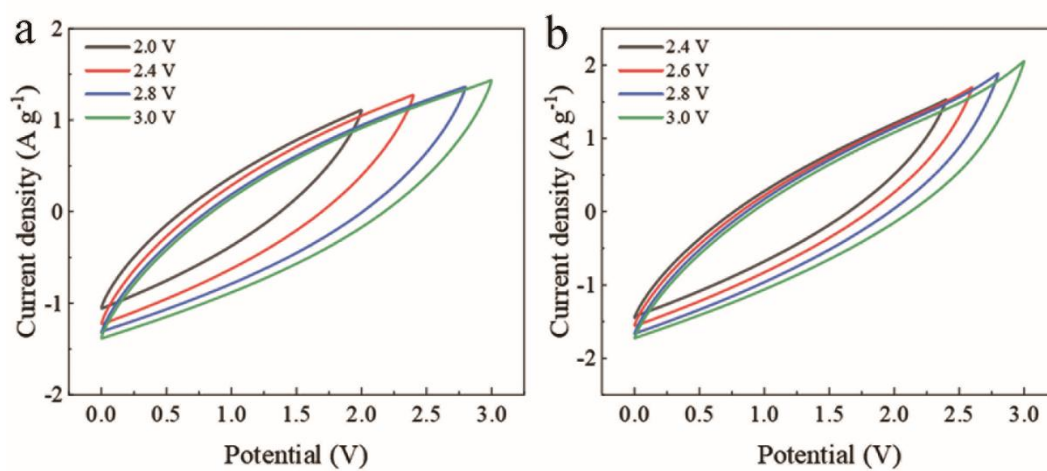
Fig. S20 CV curves of the supercapacitor using 5 and 7 mol kg^{-1} LiTFSI/H$_2$O electrolyte with different working voltage at 100 mV s^{-1} under -50 and -45 °C, respectively.

Tab. S1 Comparison of the energy densities of this work with the reported various aqueous supercapacitors.

System	Electrolyte	working voltage (V)	Energy density (Wh kg^{-1})	Ref.
TiO$_2$//MnO$_2$	1 mol L^{-1} LiClO$_4$/H$_2$O	0~2.0	7.7	[2]
AC//AC	5 mol L^{-1} LiTFSI/H$_2$O	0~2.4	10	[3]
AC//AC	5 mol kg^{-1} LiTFSI/(H$_2$O+AN)	0~2.2	11.9 (0 °C)	[4]
RPC//RPC	20 mol kg^{-1} LiTFSI/H$_2$O	0~2.4	12 (25 °C)	[5]
AB//AB	7 mol kg^{-1} LiTFSI/(H$_2$O+PC)	0~2.8	13.8	[6]
AC//AC	75 wt.% KAC/H$_2$O	0~2.0	16.8	[7]
AC//AC	17 mol kg^{-1} NaClO$_4$/H$_2$O	0~2.3	23.7	[8]
AC//AC	31.3 mol kg^{-1} LiTFSI/H$_2$O	0~2.4	30.4	[1]
NOPC//NOPC	7 mol kg^{-1} LiTFSI/H$_2$O	0~2.2	30.5	[9]
AC//AC	21 mol kg^{-1} LiTFSI/H$_2$O	0~2.42	29.24 (25 °C)	This work
AC//AC	10 mol kg^{-1} LiTFSI/H$_2$O	0~2.67	38.35 (-10 °C)	This work

References

1   P. Lannelongue, R. Bouchal, E. Mourad, C. Bodin, M. Olarte, S. le Vot, F. Favier and O. Fontaine, *J. Electrochem. Soc.*, 2018, **165**, A657-A663.

2   J. Gu, C. Jin, Z. Bian, X. Liu, S. Li, S. Tang and D. Yuan, *J. Nanopart. Res.*, 2017, **19**, 322-331.

3   G. Hasegawa, K. Kanamori, T. Kiyomura, H. Kurata, T. Abe and K. Nakanishi, *Chem. Mater.*, 2016, **28**, 3944-3950.

4   Q. Dou, S. Lei, D.-W. Wang, Q. Zhang, D. Xiao, H. Guo, A. Wang, H. Yang, Y. Li, S. Shi and X. Yan, *Energy Environ. Sci.*, 2018, **11**, 3212-3219.

5   S.-W. Xu, M.-C. Zhang, G.-Q. Zhang, J.-H. Liu, X.-Z. Liu, X. Zhang, D.-D. Zhao, C.-L. Xu and Y.-Q. Zhao, *J. Power Sources*, 2019, **441**, 227220.

6   C. Dong, W. Kang and C. An, *New J. Chem.*, 2020, **44**, 556-561.

7   Z. Tian, W. Deng, X. Wang, C. Liu, C. Li, J. Chen, M. Xue, R. Li and F. Pan, *Funct. Mater. Lett.*, 2018, **10**, 1750081.

8   X. Bu, L. Su, Q. Dou, S. Lei and X. Yan, *J. Mater. Chem. A*, 2019, **7**, 7541-7547.

9   J. Yan, D. Zhu, Y. Lv, W. Xiong, M. Liu and L. Gan, *Chin. Chem. Lett.*, 2020, **31**, 579-582.